Palmitoylation is the switch that assigns calnexin to quality control or ER Ca^{2+} signaling

Emily M. Lynes[1], Arun Raturi[1], Marina Shenkman[2], Carolina Ortiz Sandoval[1], Megan C. Yap[1], Jiahui Wu[3], Aleksandra Janowicz[1], Nathan Myhill[1], Matthew D. Benson[1], Robert E. Campbell[3], Luc G. Berthiaume[1], Gerardo Z. Lederkremer[2] and Thomas Simmen[1,*]

[1]Department of Cell Biology, University of Alberta, Edmonton, AB T6G 2H7, Canada
[2]Department of Cell Research and Immunology, George Wise Faculty of Life Sciences, Tel Aviv University, Tel Aviv 69978, Israel
[3]Department of Chemistry, University of Alberta, Edmonton, AB T6G 2G2, Canada
*Author for correspondence (Thomas.Simmen@ualberta.ca)

Accepted 10 June 2013
Journal of Cell Science 126, 3893–3903

doi: 10.1242/jcs.125856

Summary

The palmitoylation of calnexin serves to enrich calnexin on the mitochondria-associated membrane (MAM). Given a lack of information on the significance of this finding, we have investigated how this endoplasmic reticulum (ER)-internal sorting signal affects the functions of calnexin. Our results demonstrate that palmitoylated calnexin interacts with sarcoendoplasmic reticulum (SR) Ca^{2+} transport ATPase (SERCA) 2b and that this interaction determines ER Ca^{2+} content and the regulation of ER–mitochondria Ca^{2+} crosstalk. In contrast, non-palmitoylated calnexin interacts with the oxidoreductase ERp57 and performs its well-known function in quality control. Interestingly, our results also show that calnexin palmitoylation is an ER-stress-dependent mechanism. Following a short-term ER stress, calnexin quickly becomes less palmitoylated, which shifts its function from the regulation of Ca^{2+} signaling towards chaperoning and quality control of known substrates. These changes also correlate with a preferential distribution of calnexin to the MAM under resting conditions, or the rough ER and ER quality control compartment (ERQC) following ER stress. Our results have therefore identified the switch that assigns calnexin either to Ca^{2+} signaling or to protein chaperoning.

Key words: Endoplasmic reticulum, Mitochondria, Quality control, Ca^{2+} signaling, ERp57, SERCA2b

Introduction

The main functions of the endoplasmic reticulum (ER) are the production of secretory and membrane proteins as well as lipids, and the storage of Ca^{2+}. An integral requirement for these functions is the interaction of the ER with mitochondria, which occurs on the mitochondria-associated membrane (MAM), a subdomain of the ER that makes close contacts between the ER and the mitochondria (Raturi and Simmen, 2013; Simmen et al., 2010). Here, the ER exchanges Ca^{2+} with mitochondria through the ER Ca^{2+}-handling inositol (1,4,5)-triphosphate receptors (IP3R) and the sarcoendoplasmic reticulum (SR) Ca^{2+} transport ATPase (SERCA) (Rizzuto et al., 2009). Under resting conditions, Ca^{2+} delivery from the ER to the mitochondrial matrix is needed to activate the mitochondrial enzyme pyruvate dehydrogenase (PDH), which drives the tricarboxylic acid (TCA) cycle (Cárdenas et al., 2010). Given the crucial role that mitochondrial metabolism plays in death and survival of the cell (Glancy and Balaban, 2012; Zhivotovsky and Orrenius, 2011), ER–mitochondria Ca^{2+} exchange has to be regulated at the source. Various ER chaperones and oxidoreductases perform this function by dictating Ca^{2+} channels and pumps to open or close dependent on ER redox and Ca^{2+} homeostasis (Simmen et al., 2010). Examples are Ero1α, which activates IP3Rs (Li et al., 2009), and ERp44, which inhibits IP3Rs (Higo et al., 2005).

Calnexin is another key ER chaperone that binds to nascent glycoproteins (Rutkevich and Williams, 2011). This binding slows down client protein folding and prevents their aggregation owing to retention of folding intermediates in the ER. Upon release from calnexin, glycoproteins can follow one of three pathways: they might fold rapidly and correctly, in which case they will be exported to the Golgi apparatus, or if they are not yet correctly folded they can be re-glucosylated and returned to the calnexin cycle (Ruddock and Molinari, 2006). Proteins that have been trapped in the calnexin cycle for a prolonged period are eventually subject to extensive mannose trimming by mannosidase I and ER-associated degradation enhancing α-mannosidase-like protein (EDEM), followed by retrotranslocation from the ER to the cytosol and degradation by the proteasome, a process known as ER-associated degradation (ERAD) (Lederkremer, 2009). All along, calnexin works in partnership with ERp57, an oxidoreductase that is a member of the protein disulfide isomerase (PDI) family (Coe and Michalak, 2010; Oliver et al., 1997; Zapun et al., 1998). Studies have shown that a certain subset of disulfide-bonded heavily glycosylated proteins such as the low-density lipoprotein receptor (LDLR) depend specifically on this partnership for efficient folding and subsequent trafficking through the secretory system (Jessop et al., 2007; Rutkevich and Williams, 2011).

Surprisingly, our laboratory and others have determined that calnexin is not only found on the rough ER, but is often enriched on the MAM (Hayashi and Su, 2007; Myhill et al., 2008; Wieckowski et al., 2009). This finding further reinforces the notion that calnexin is a central player for the regulation of ER Ca^{2+} signaling, and is also consistent with the fact that calnexin

interacts with the SERCA Ca^{2+} pump (Roderick et al., 2000). Interestingly, the role of calnexin in Ca^{2+} signaling could depend on ER homeostasis, given that ER stress results in the relocation of calnexin towards the ER quality control compartment (ERQC) and its association with slowly folding proteins (Frenkel et al., 2004).

Therefore, we have examined whether the targeting of calnexin to different ER subdomains correlates with an ER-stress-dependent role in ER Ca^{2+} signaling towards mitochondria. We further examined whether such a role correlated with the extent of binding of calnexin to its known partners ERp57 and SERCA2b. Calnexin targeting to the MAM depends on a juxtamembrane palmitoylation motif (Lynes et al., 2012) that is implicated in mediating the interaction of calnexin with the translocon (Lakkaraju et al., 2012) and with lipid rafts on the plasma membrane (Ferrera et al., 2008). In addition to calnexin, palmitoylation is known to modify several ER proteins, including heme oxygenase-1 and ORAI1, but the consequences of this modification are currently unknown (Dowal et al., 2011; Kang et al., 2008). We had shown earlier that the interference with palmitoylation relocates heme oxygenase-1 (Lynes et al., 2012), but ER-associated palmitoylation might have multiple diverse effects (Lakkaraju et al., 2012). To investigate the functional significance of palmitoylation-dependent targeting of calnexin, we characterized the functional consequences of the palmitoylation state of calnexin for the cell in terms of cellular Ca^{2+} signaling and quality control of the known calnexin substrates LDLR and asialoglycoprotein receptor (ASGPR).

Results

ER stress affects the palmitoylation of calnexin and its localization within the ER

To test whether ER stress influences the function of calnexin in ER Ca^{2+} signaling and chaperoning, we first examined the localization of calnexin following ER stress by biochemical fractionation. We decided to separate ER membranes into light and heavy membranes. Using this technique, we detected a shift of calnexin towards light membranes that started after 1 h of tunicamycin treatment and increased at 4 h (Fig. 1A). No such shift was observed for PDI or BAP31 (data not shown), two other ER proteins. To more precisely determine the origin and destination of calnexin during short-term ER stress, we used a

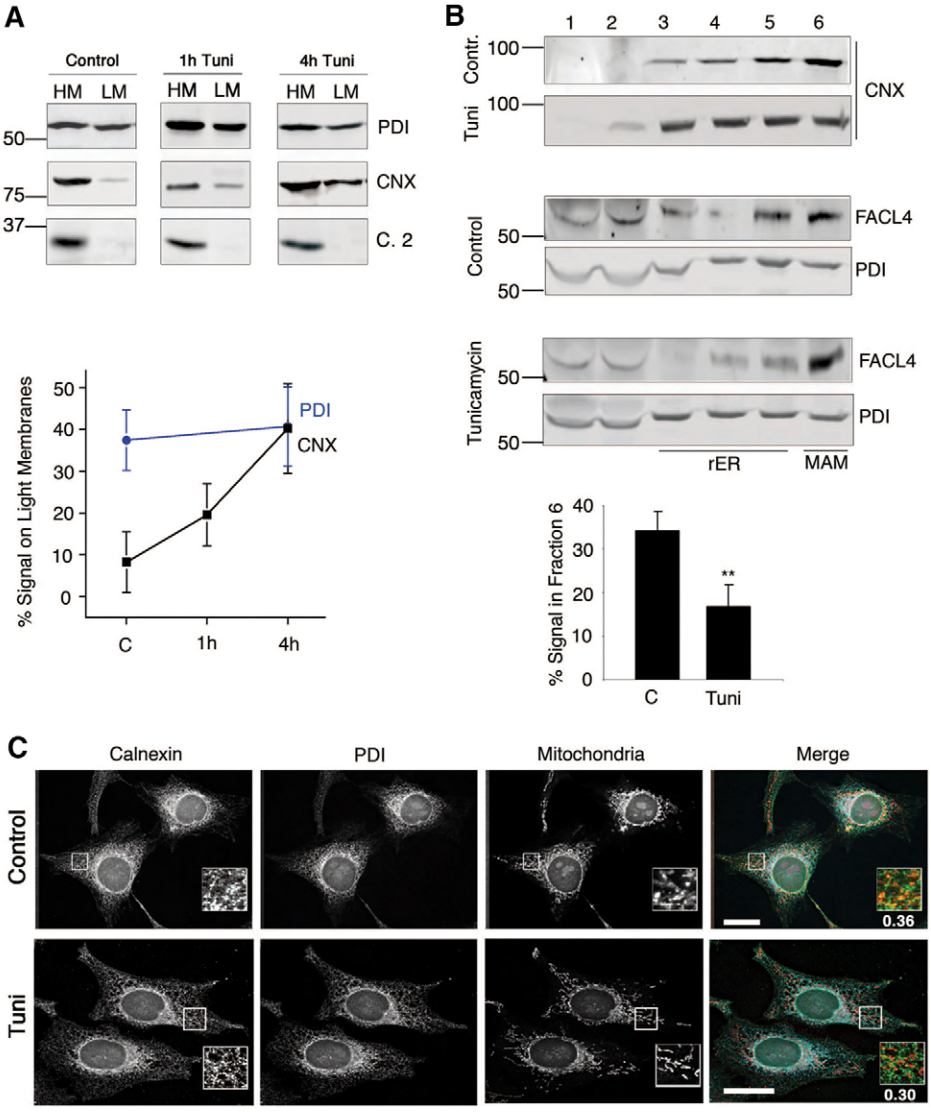

Fig. 1. ER stress affects the ER internal distribution of calnexin. (**A**) Heavy and light membrane fractionation (HM and LM, respectively) following ER stress. Homogenized HeLa cell lysates were separated into heavy and light membranes following a 1 h or 4 h treatment with 10 µM Tunicamycin (Tuni). Membrane fractions were analyzed as indicated by SDS-PAGE and western blot for PDI, calnexin (CNX) and mitochondrial complex 2 (C. 2). The graph shows the distribution time course for PDI and calnexin. C, control (before treatment). (**B**) Optiprep fractionation following ER stress. Homogenized HeLa cell lysates were separated by Optiprep following a 4 h treatment with 10 µM Tunicamycin into six fractions. Membrane fractions were analyzed as indicated by SDS-PAGE and western blotting for PDI (pan-ER) and FACL4 (MAM), as well as calnexin. The graph shows the calnexin amount in the MAM fraction (fraction six) from three independent experiments. $^{**}P=0.035$. (**C**) The calnexin signal proximal to mitochondria depends on ER stress. Control HeLa cells and cells treated with 10 µM Tunicamycin were processed for immunofluorescence microscopy as described and analyzed for the signals of calnexin, PDI and mitochondria (mitotracker). The merged images (calnexin, green; PDI, blue; mitochondria, red) are shown on the right with a zoomed area of just calnexin and mitotracker signals (inset). Manders coefficients: 0.36 for wild-type endogenous calnexin under control conditions, 0.30 for wild-type, endogenous calnexin following 4 h 10 µM Tunicamycin treatment (from 14 cells each). Scale bars: 25 µm.

biochemical fractionation technique that we had developed to separate MAM markers from other ER markers (Myhill et al., 2008). HeLa cells were treated with two different ER stressors, thapsigargin and tunicamycin, for 4 h, then homogenized and fractionated using Optiprep density gradient medium (Fig. 1B; supplementary material Fig. S1, Fig. S2A). The general ER marker PDI and MAM-localized long-chain acyl-CoA ligase 4 (FACL4) were used to control for the sedimentation of the MAM compartment. Under control conditions, close to 40% of calnexin co-fractionates with the MAM marker FACL4 and with the mitochondria at the bottom of the Optiprep gradient, as previously shown by our laboratory and others. However, after treatment with ER stressors, the association of calnexin, but not of PDI or FACL4 with MAM fractions was diminished to less than 20%. The relocation of calnexin did not lead to increased targeting to the plasma membrane (data not shown). Immunofluorescence microscopy similarly suggested reduced apposition between calnexin and mitochondria (Fig. 1C). After 4 h of treatment with tunicamycin, a decrease in the overlap of the calnexin and mitotracker signals was observed (yellow signal, inset box) in HeLa cells labeled with antibodies against calnexin and PDI, as well as mitotracker. This result is consistent with a decrease in the localization of calnexin at the MAM. At first glance, the relocation of calnexin away from mitochondria during ER stress appears surprising, given earlier reports by us and others that this condition increases visible contacts between ER and mitochondria (Bravo et al., 2011; Csordás et al., 2006). At the same time, however, this movement of calnexin away from the MAM suggests a specific function that is not due to known structural changes in the ER.

Next, we aimed to identify the mechanism that could lead to this relocation of calnexin. Because the phosphorylation state of calnexin is important for its localization within the ER and its binding to PACS-2 (Myhill et al., 2008), we tested the status of phosphorylation for each known site during an ER stress timecourse. Our results ruled out that a change in phosphorylation is behind the relocation of calnexin, given that only long-term, but not short-term, stress led to a reduction of calnexin phosphorylation on serine 565, which controls PACS-2 binding, and serine 584 (Fig. 2A), which controls the interaction of calnexin with ribosomes and SERCA2b (Chevet et al., 1999; Roderick et al., 2000). Another explanation for the change in localization of calnexin during short-term ER stress could be that calnexin loses its palmitoylation, known to be responsible for its MAM targeting (Lynes et al., 2012). Thus, we used a 'click chemistry' approach to compare the calnexin palmitoylation signal from untreated cells to that of cells treated with tunicamycin or DTT for 4 h to induce a short-term ER stress (Fig. 2B; supplementary material Fig. S2B). We observed that both ER stress situations indeed led to calnexin depalmitoylation. Therefore, in contrast to long-term ER stress (Delom et al., 2007), short-term ER stress results in calnexin depalmitoylation, but not dephosphorylation, together with a loss of MAM enrichment.

Short-term ER stress affects the interactions between calnexin and SERCA2b

Next, we aimed to test whether the relocation of calnexin within the ER that occurs in parallel with its depalmitoylation also affects its key interactors, because such an observation could give clues as to what palmitoylation of calnexin is necessary for.

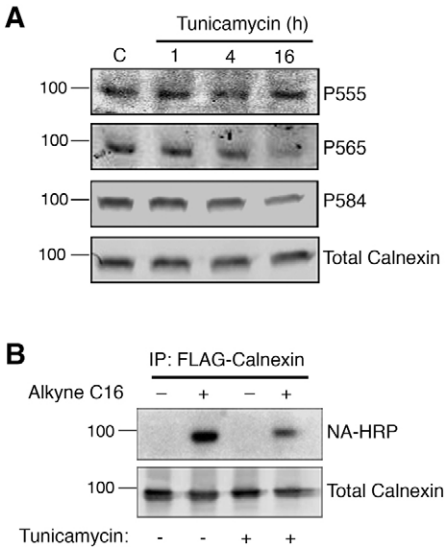

Fig. 2. Analysis of calnexin phosphorylation and palmitoylation during an ER stress time course. (**A**) Calnexin phosphorylation at its three sites is individually altered during an ER stress time course. HeLa cells treated for the indicated times with 10 µM Tunicamycin were snap-lysed with sample buffer and analyzed by western blotting using phospho-specific antibodies against each of the three known sites of phosphorylation – serine 555, 565, 584 (dog nomenclature). C, control (before treatment). (**B**) Calnexin palmitoylation is reduced during ER stress. HeLa cells were incubated for 4 h with 10 µM Tunicamycin and then processed for click chemistry as described previously (Lynes et al., 2012).

Because calnexin interacts with SERCA2b (Roderick et al., 2000), we decided to first test whether treatment with ER stressors also affects SERCA2b. Thus, we examined the distribution of SERCA2b on our Optiprep gradient, as well as on heavy versus light membranes. Whereas calnexin moved away from the MAM and heavy membranes of the ER, we could, however, not detect any movement of SERCA2b under these conditions (Fig. 3A). This suggested that calnexin and SERCA2b undergo different fates during ER stress.

To test this hypothesis, we immunoprecipitated calnexin from control HeLa cells and HeLa cells treated with either DTT or tunicamycin for 4 h. Under these ER stress conditions, we found that the interaction of calnexin with SERCA2b decreased significantly (Fig. 3B). The replacement of the two cysteine residues of calnexin that are subject to palmitoylation with alanine residues (cysteine 503 and 504 in dog calnexin, CCAA) resulted in a similar reduction of the SERCA2b–calnexin interaction (Fig. 3C). Calnexin phosphorylation on serine 584 had previously been implicated in the regulation of this interaction with SERCA2b (Roderick et al., 2000). However, we could not detect reduction of phosphorylation on this residue within the time frame that led to reduction of the SERCA2b–calnexin interaction. Consistent with these findings, we could also not detect reduced phosphorylation of calnexin in a mutant where we had replaced the two membrane-proximal cysteine residues with alanine residues (CCAA), resulting in non-palmitoylatable calnexin (Lynes et al., 2012) (supplementary material Fig. S2C). Taken together, our results demonstrate that short-term ER stress results in the depalmitoylation of calnexin, but not its dephosphorylation. Calnexin depalmitoylation subsequently results in reduced association of calnexin with SERCA2b.

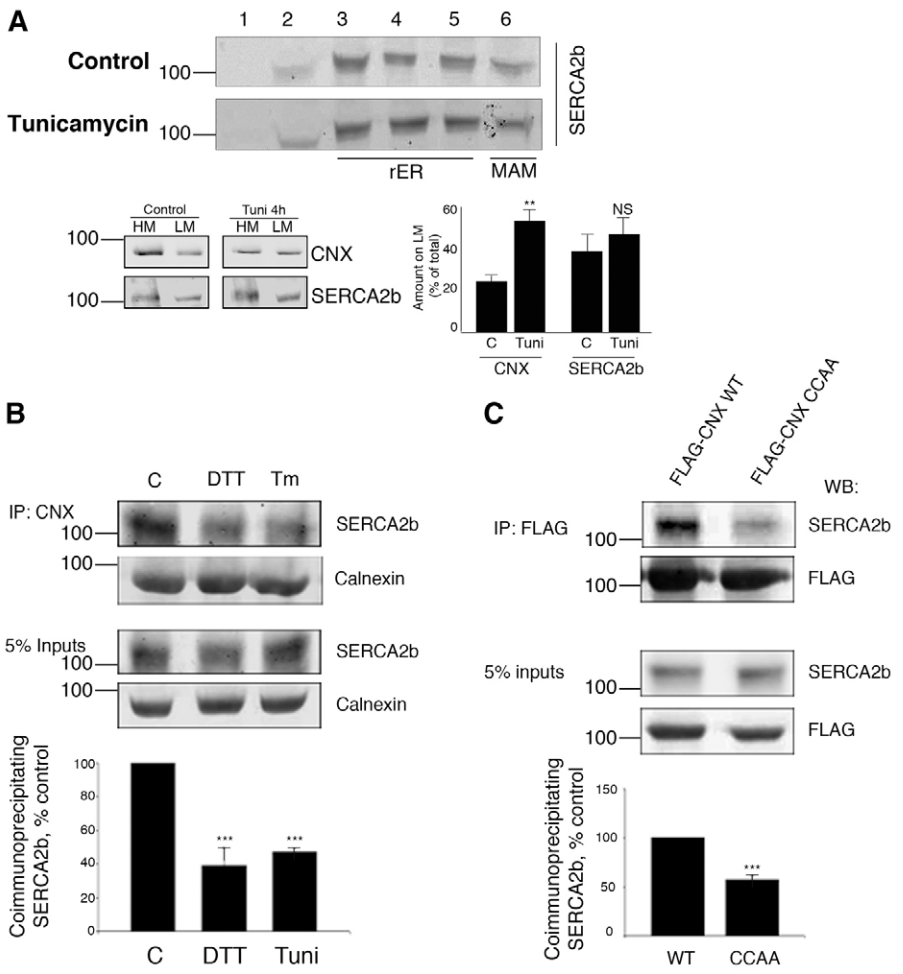

Fig. 3. ER stress and palmitoylation affect the interaction between calnexin and SERCA2b. (**A**) Optiprep and membrane fractionation following ER stress. Homogenized HeLa cell lysates were separated using Optiprep, following a 4 h treatment with 10 µM Tunicamycin (Tuni), into six fractions. Membrane fractions were analyzed as indicated by SDS-PAGE and western blotting for SERCA2b (upper panel). Lower left panel: homogenized HeLa cell lysates were separated into heavy and light membranes (HM and LM, respectively) following a 4 h treatment with 10 µM Tunicamycin. Membrane fractions were analyzed as indicated by SDS-PAGE and and western blotting for calnexin (CNX) and SERCA2b. The graph shows the calnexin and SERCA2b amounts in the heavy membrane fraction from three independent experiments. C, control (before treatment). $^{**}P=0.013$ for calnexin; $P=0.395$ (NS) for SERCA2b. (**B**) Calnexin–SERCA2b co-immunoprecipitation following ER stress. HeLa cells were treated for 4 h with either 2 mM Dithiothreitol (DTT) or 10 µM Tunicamycin. DSP-crosslinked lysates (5% inputs) and calnexin immunoprecipitates (IP: CNX) were analyzed for calnexin and co-immunoprecipitating SERCA2b. The graph shows results from three independent experiments ($^{***}P=0.0073$ for DTT, $^{***}P<0.001$ for Tunicamycin). (**C**) Calnexin and the calnexin palmitoylation mutant (CNX CCAA) co-immunoprecipitation with SERCA2b. HeLa cells were transfected with FLAG-tagged wild-type or CCAA calnexin. DSP-crosslinked lysates (5% inputs) and FLAG immunoprecipitates (IP: FLAG) were analyzed for FLAG-tagged calnexin and co-immunoprecipitating SERCA2b. The graph shows results from three independent experiments. $^{***}P=0.006$.

Calnexin palmitoylation allows for controlled ER–mitochondria Ca^{2+} transfer

Our results suggested that palmitoylated calnexin might regulate ER Ca^{2+} signaling. If this were correct we would expect palmitoylated calnexin to regulate the flux of Ca^{2+} between the ER and mitochondria through its role on SERCA (Roderick et al., 2000). Thus, we performed an extensive series of Ca^{2+} assays using calnexin-knockout mouse embryonic fibroblasts (MEFs) (Kraus et al., 2010) that we transfected with wild-type and non-palmitoylatable calnexin. First, we inhibited SERCA Ca^{2+} pumps with thapsigargin and measured the increase of cytosolic Ca^{2+} with Fluo8. We were unable to detect any differences in the accumulation of cytosolic Ca^{2+} with this assay, regardless of whether palmitoylated or non-palmitoylated calnexin was present or not (Fig. 4A). No change in the accumulation of cytosolic Ca^{2+} was observed using FURA-2 either (supplementary material Fig. S3A). These results were consistent with earlier reports (Zuppini et al., 2002). However, we decided to measure ER Ca^{2+} at the source using ER-targeted aequorin (Alvarez and Montero, 2002). Surprisingly, our measurements showed ~80% more Ca^{2+} in MEFs transfected with wild-type calnexin, but not with calnexin that cannot be palmitoylated (Fig. 4B). Because these cells did not show altered accumulation of cytosolic Ca^{2+} from ER stores, our findings suggested that mitochondrial Ca^{2+} uptake could also be different in cells expressing calnexin compared with that in calnexin-knockout MEFs (Arnaudeau et al., 2001; de Brito and Scorrano, 2008). Therefore, we tested whether mitochondria show differences in Ca^{2+} uptake following the inhibition of ER Ca^{2+} pumps. Indeed, we found that mitochondria in wild-type MEFs take up significantly less Ca^{2+} than calnexin-knockout MEFs (supplementary material Fig. S3B). Moreover, our results with the mitochondrial Ca^{2+} indicator dye Rhod2 in the presence of thapsigargin show that the presence of wild-type calnexin dampened mitochondrial Ca^{2+} uptake following thapsigargin administration, when compared with that in calnexin-knockout MEFs (Fig. 4C). Importantly, this effect was not seen using non-palmitoylated calnexin. Because our results indicate that the presence of palmitoylated calnexin reduced the ability of mitochondria to import Ca^{2+} from the ER, we next tested whether this was also true under the condition of ER stress, when cells normally increase mitochondrial Ca^{2+} import from ER sources (Bravo et al., 2011; Csordás et al., 2006). Our results show that calnexin-knockout MEFs were unable to boost the import of IP3R-released Ca^{2+} into mitochondria after a 4 h tunicamycin stress. However, the transfection of wild-type calnexin, but not of non-palmitoylatable calnexin rescued this deficiency (Fig. 4D), thus making calnexin-knockout MEFs stress-responsive again. Taken together, our results suggest that calnexin must be palmitoylatable to control the activity of SERCA and thus the rate of Ca^{2+} import into mitochondria.

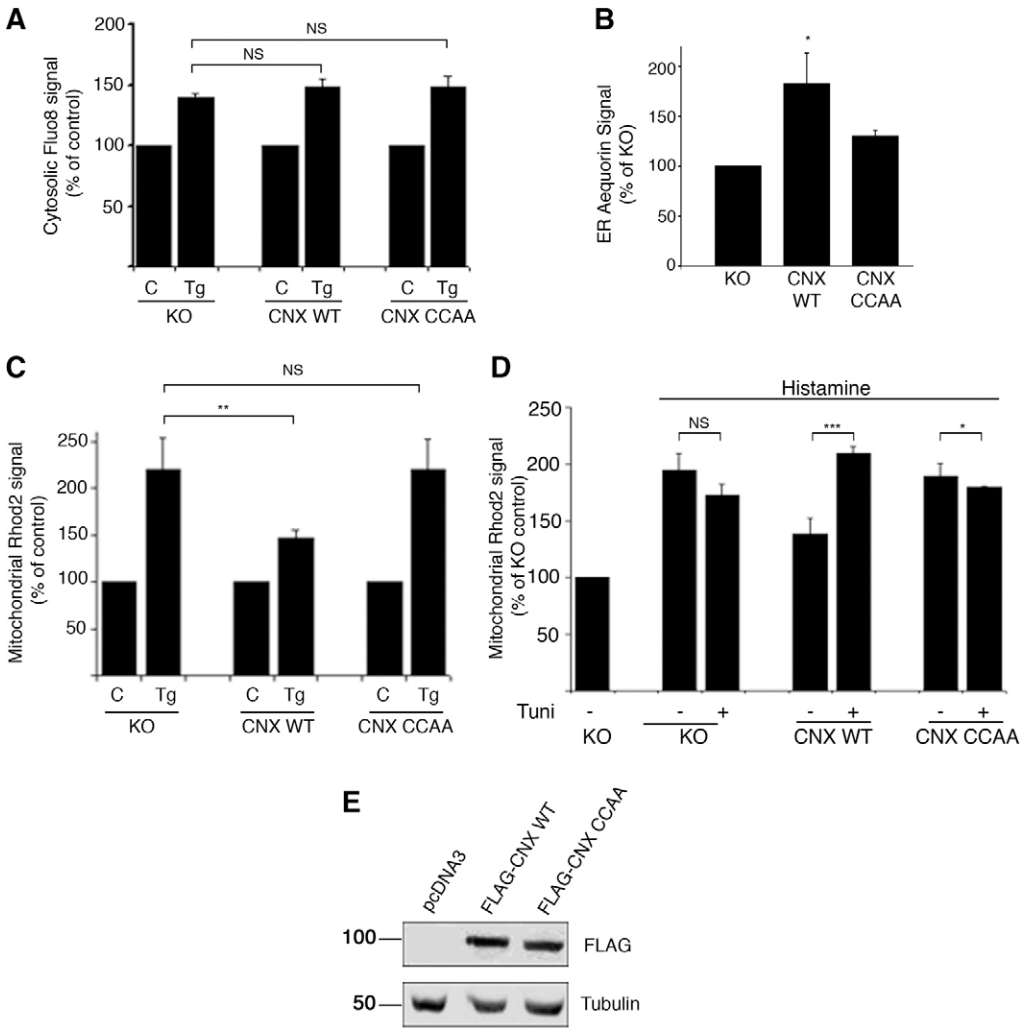

Fig. 4. Palmitoylated calnexin regulates ER Ca^{2+} signaling. (**A**) Measurement of cytosolic Ca^{2+} following thapsigargin (Tg)-mediated ER Ca^{2+} release. Calnexin (CNX) knockout (KO) MEFs and KO cells transfected with FLAG-tagged wild-type (WT) or CCAA calnexin were loaded with Fluo8. Cells were then treated with 1.5 µM thapsigargin and probe fluorescence was recorded before and after thapsigargin treatment by flow cytometry. C, control (before treatment). $P=0.8419$ for calnexin wild-type (NS), $P=0.8816$ for calnexin CCAA (NS). (**B**) Measurement of ER Ca^{2+} content. Calnexin knockout (KO) MEFs and KO cells transfected with FLAG-tagged wild-type or CCAA calnexin were co-transfected with a plasmid encoding ER-targeted aequorin. Luminescence was plotted from three independent experiments following the protocol outlined in the Materials and Methods. *$P=0.08$ (**C**) Measurement of mitochondrial Ca^{2+} following thapsigargin-mediated ER Ca^{2+} release. Calnexin knockout (KO) MEFs and KO cells transfected with FLAG-tagged wild-type or CCAA calnexin were loaded with Rhod2. Cells were then treated with 1.5 µM thapsigargin and probe fluorescence was recorded before and after thapsigargin treatment by flow cytometry. **$P=0.02$ for calnexin wild-type, $P=0.8583$ for calnexin CCAA (NS). (**D**) Measurement of mitochondrial Ca^{2+} following histamine-mediated ER Ca^{2+} release. Calnexin knockout (KO) MEFs and KO cells transfected with FLAG-tagged wild-type or CCAA calnexin were loaded with Rhod2. Cells were then treated with 50 µM histamine and probe fluorescence was recorded before and after histamine treatment by flow cytometry ($P=0.2581$ for calnexin knockout (NS), ***$P<0.001$ for calnexin wild-type, *$P=0.088$ for calnexin CCAA). (**E**) Calnexin expression levels of representative cells from flow cytometry experiments. Calnexin knockout (KO) MEFs and KO cells transfected with FLAG-tagged wild-type or CCAA calnexin were lysed and processed for western blotting using the FLAG antibody.

Given that efficient Ca^{2+} transfer from the ER to mitochondria is a prerequisite for the mitochondrial membrane potential (Cárdenas et al., 2010), we next tested the hypothesis that calnexin-knockout cells could exhibit an abnormally high proton gradient across the mitochondrial membranes owing to their high constitutive Ca^{2+} transfer from the ER to mitochondria. By labeling calnexin-knockout cells and their counterparts transfected with wild-type calnexin and non-palmitoylatable calnexin with tetramethylrhodamine methyl ester (TMRM), we were indeed able to confirm this hypothesis by demonstrating that only wild-type calnexin transfection resulted in a specific reduction of the mitochondrial membrane potential (supplementary material Fig. S3C). This was also the case in the presence of KCl, which equilibrates plasma membrane uptake of TMRM (data not shown). Throughout our experiments, we verified that expression of the two calnexin constructs was even (Fig. 4E) and that our transfections did not result in the induction of the unfolded protein response (supplementary material Fig. S3D). Therefore, ER–mitochondria Ca^{2+} transfer is more efficient in the absence of calnexin, but the boosted Ca^{2+} transfer observed under ER stress requires palmitoylated calnexin and increases the ER Ca^{2+} content.

The palmitoylation state of calnexin regulates its interaction with ERp57

In addition to its interaction with SERCA2b, calnexin interacts with the oxidoreductase ERp57 in the ER to mediate protein folding. This role of calnexin is particularly important for slow-folding substrates (Frenkel et al., 2004). Thus, we decided to also test whether the interaction between calnexin and ERp57 is similarly affected by ER stress. First, we examined the distribution of calnexin and ERp57 by Optiprep gradient and fractionation of cellular membranes into heavy and light membranes. In contrast to SERCA2b (Fig. 3A), the distribution of ERp57 closely matched that of calnexin and both turned out to move from heavy to light membranes following an ER stress (Fig. 5A), suggesting that these two proteins might share functions under ER stress. Indeed, we observed that when cells are treated with either DTT or tunicamycin for 4 h, the amount of interaction between calnexin and ERp57 increased (Fig. 5B). ER stress could lead to the misfolding of calnexin itself, which could then trigger its association with other chaperones. To test this possibility, we expressed FLAG-tagged calnexin and the mutant calnexin that cannot be palmitoylated. As shown in Fig. 5C, the calnexin CCAA mutant that cannot be palmitoylated indeed

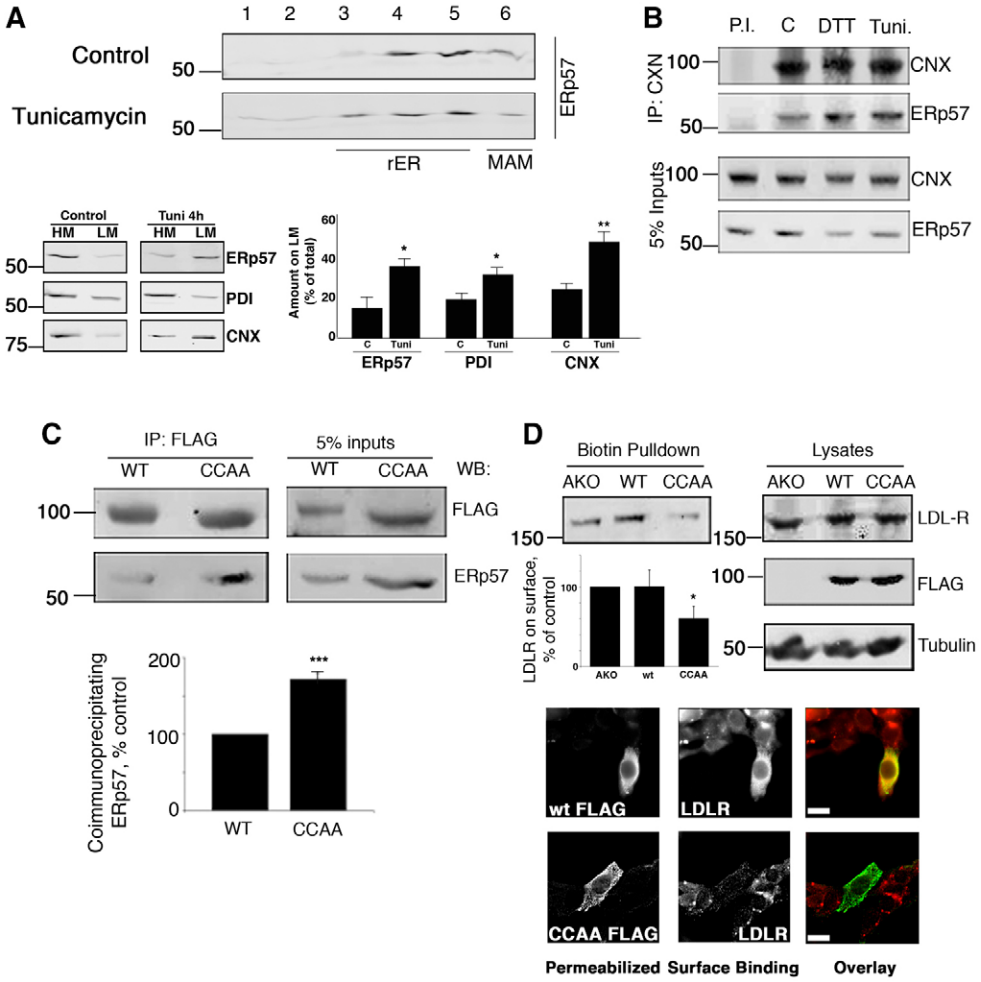

Fig. 5. ER stress and palmitoylation affect the interaction between calnexin and ERp57. (**A**) Optiprep and membrane fractionation following ER stress. Homogenized HeLa cell lysates were separated using Optiprep, following a 4 h treatment with 10 µM Tunicamycin (Tuni), into six fractions. Membrane fractions were analyzed as indicated by SDS-PAGE and western blotting for ERp57, PDI and calnexin (upper panel). Lower left panel: homogenized HeLa cell lysates were separated into heavy and light membranes (HM and LM, respectively) following a 4 h treatment with 10 µM Tunicamycin. Membrane fractions were analyzed as indicated by SDS-PAGE and western blotting for ERp57, PDI and calnexin (CNX). The graph shows the ERp57, PDI and calnexin amounts in the heavy membrane fraction from three independent experiments. C, control (without treatment). $*P=0.056$ for ERp57, $*P=0.088$ for PDI, $**P=0.013$ for calnexin. (**B**) Calnexin–ERp57 co-immunoprecipitation following ER stress. HeLa cells were treated for 4 h with either 2 mM Dithiothreitol (DTT) or 10 µM Tunicamycin. DSP-crosslinked lysates (5% inputs) and calnexin immunoprecipitates (IP: CNX) were analyzed for calnexin and co-immunoprecipitating ERp57. (**C**) Calnexin and the calnexin palmitoylation mutant (CCAA)–ERp57 co-immunoprecipitation. HeLa cells were transfected with FLAG-tagged wild-type (WT) or CCAA calnexin. DSP-crosslinked lysates (5% inputs) and FLAG immunoprecipitates were analyzed for FLAG-tagged calnexin and co-immunoprecipitating ERp57. The graph shows results from three independent experiments. $***P=0.003$. (**D**) LDLR surface biotinylation. Calnexin knockout (KO) MEFs and KO cells transfected with FLAG-tagged wild-type or CCAA calnexin were lysed and processed for western blotting using the anti-LDLR antibody. In parallel, the same set of cells was processed for surface biotinylation as described in the Materials and Methods and probed for biotinylated surface LDLR. The bar graph shows the means of three independent experiments. $*P=0.07$. Cells were also processed for LDLR surface binding, followed by permeabilization and detection of intracellular transfected FLAG-tagged calnexin as shown in the lower images. Scale bars: 25 µm.

interacted with ERp57 almost twice as well. Likewise, the binding of calnexin to ERp57 was approximately doubled in the presence of 2-bromopalmitate, an inhibitor of palmitoylation (supplementary material Fig. S4A).

Our results suggested that the change in the interaction between calnexin and ERp57 that was dependent on palmitoylation is of a functional nature. We therefore sought to identify a folding substrate that is particularly dependent on the calnexin–ERp57 folding pathway. For this purpose, we first chose the LDLR, which is known to undergo protein folding by forming mixed disulfides with ERp57 and depend on calnexin folding (Jessop et al., 2007). To determine whether LDLR maturation proceeds differently when calnexin is palmitoylated or not, we used the calnexin-knockout MEFs that we transfected with wild-type calnexin or the calnexin CCAA mutant. Despite the expression level of the LDLR in cell lysates being unaltered (Fig. 5D), we found that the amount of LDLR on the cell surface increased when wild-type calnexin was expressed, but decreased when CCAA calnexin was expressed (Fig. 5D), suggesting that non-palmitoylated calnexin is indeed more stringent in ER quality control retention than the at least partially palmitoylated wild-type calnexin.

Efficient intracellular retention of LDLR by non-palmitoylated calnexin could indicate that this form of calnexin interacts with unfolded domains of proteins that await exit from the ER or, alternatively, ER-associated degradation (ERAD). Thus, we analyzed the interaction of calnexin with an ERAD substrate, the uncleaved precursor of asialoglycoprotein receptor (ASGPR) H2a, which is normally completely retained in the ER (Kamhi-Nesher et al., 2001; Shenkman et al., 1997). Calnexin CCAA interacted much more robustly than wild-type CNX with H2a (Fig. 6A). Calnexin CCAA also caused a slight increase in total H2a, probably because of decreased targeting of this protein for ERAD. Pulse-chase analysis showed that dissociation of H2a from calnexin followed a different pattern when we transfected nonpalmitoylatable calnexin compared with upon transfection of wild-type calnexin (Fig. 6B). Whereas wild-type calnexin dissociated efficiently with time from the ERAD substrate H2a, non-palmitoylatable CCAA calnexin reassociated and remained in a complex with H2a for extended periods of time. For the pulse samples, two bands can be seen for H2a precursor molecules, the lower one corresponding to an underglycosylated species (one of the glycosylation sites unoccupied). As we had shown previously (Frenkel et al., 2004), the fully glycosylated species shifts progressively to a faster migration because of the trimming of mannose residues on its N-glycans, whereas the underglycosylated lower species is quickly degraded.

We next tested whether palmitoylation influences calnexin targeting to the pericentriolar ERQC, where calnexin and ERAD substrates like H2a accumulate upon inhibition of their degradation or under ER stress (Frenkel et al., 2004; Kamhi-Nesher et al., 2001; Kondratyev et al., 2007). Thus, we compared the localization of the non-palmitoylatable mutant with wild-type calnexin. Whereas in untreated cells, both proteins showed a disperse ER pattern, upon short-term proteasomal inhibition for 3 h, calnexin CCAA showed a more pronounced relocation to the juxtanuclear ERQC and colocalization with H2a linked to monomeric RFP (H2a–RFP), according to the Manders coefficient (Fig. 6C–F). Taken together, our results demonstrate the preferential interaction of non-palmitoylated calnexin with ERAD substrates, which extends to the ERQC, where dissociation from the misfolded glycoprotein would require the ability of calnexin to undergo palmitoylation.

Discussion

The results presented herein uncover a mechanistic description of the role of calnexin palmitoylation during ER stress. We demonstrate that reversible palmitoylation assigns calnexin to the interaction with SERCA2b and a role in the regulation of Ca^{2+} transfer to mitochondria, whereas non-palmitoylated calnexin tends to interact with ERp57 to fulfill its role in protein folding and quality control (Fig. 7). Our results therefore illustrate for the first time how palmitoylation can restrict calnexin to either role, and we propose that palmitoylation is a key mechanism of ER stress signaling. Our observations identify palmitoylation as a quick signal that reassigns calnexin to specific tasks within the ER, unlike phosphorylation, which determines calnexin interaction with the ribosome, and another ER chaperone, BAP31, in a less dynamic way. Changes in calnexin phosphorylation require significantly longer exposure to ER stress when compared to the changes in palmitoylation (Fig. 2). Moreover, whereas the calnexin phosphorylation state results in intra-ER relocations mediated by the cytosolic sorting protein PACS-2 (Myhill et al., 2008), palmitoylation might regulate the calnexin localization by allowing (or not) its interaction with its effectors SERCA2b and ERp57, which are localized to sites of Ca^{2+} signaling and protein folding, respectively. Interestingly, calnexin appears to follow a targeting pattern that is probably relatively unique, since ER and mitochondria move closer to each other during ER stress, suggesting an enrichment of ER proteins at the MAM or a tightening of ER–mitochondria contacts (Bravo et al., 2011; Csordás et al., 2006).

So far, the interaction of calnexin with its substrates has been explained from the substrate's point of view, given that calnexin binds exclusively monoglucosylated substrates (Lederkremer, 2009). This property, together with the enzymatic action of UDPGlc:glycoprotein glucosyltransferase and glucosidases I and II leads to a cyclic interaction of folding substrates with calnexin until proper folding is reached or ERAD is triggered. Our new data now indicate that calnexin itself undergoes a palmitoylation-dependent cycle within the ER and shuttles back and forth from regulating Ca^{2+} signaling at or close to the MAM and mediating protein folding and quality control at or close to the rough ER, including the targeting of unfolded or misfolded proteins to the ERQC (Leitman et al., 2013). Interestingly, these results could help explain the anti-stress function of 2-bromopalmitate (2BP) treatment, which attenuates the induction of ER stress transcription factors and the progression of apoptosis (Baldwin et al., 2012). In this scenario, calnexin would become more efficient as a chaperone and would hence mitigate the effects of any additionally introduced ER stressor. Consistent with such an idea, we observed that the inhibition of palmitoylation with 2BP leads to a 2-fold increase in the binding of ERp57 with calnexin (supplementary material Fig. S4A), increases the association with H2a and reduces the amount of mature LDLR on the surface (supplementary material Fig. S4B). These findings, together with the decreased amount of surface LDLR upon expression of CCAA calnexin, suggest that palmitoylation facilitates the dissociation of calnexin from folding intermediates.

Accordingly, palmitoylated calnexin appears to be less important for protein folding, consistent with its predominant

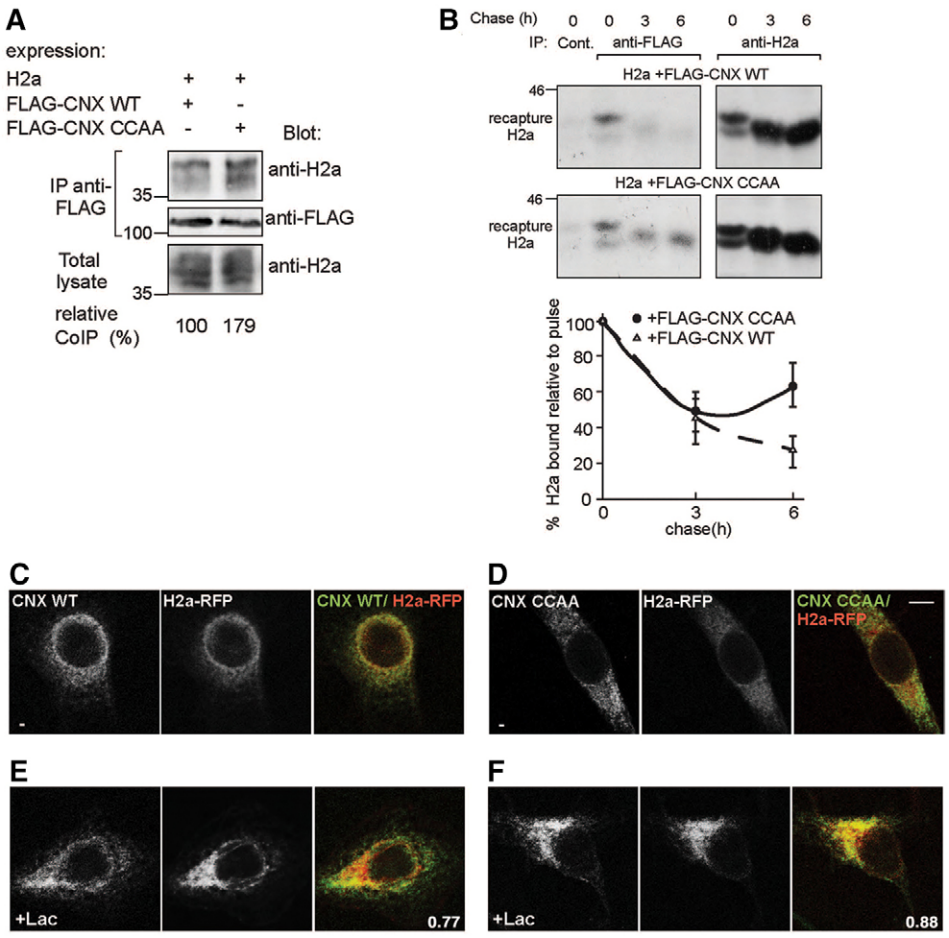

Fig. 6. Involvement of non-palmitoylated calnexin in glycoprotein quality control. (**A**) Increased interaction of an ERAD substrate with calnexin (CNX) CCAA as compared with wild-type calnexin (WT). HEK-293 cells were cotransfected with a vector encoding for an ERAD substrate glycoprotein, H2a, and FLAG-tagged CNX WT or CNX CCAA. The cells were lysed in 2% sodium cholate (Materials and Methods) and 10% of the lysates were run on 10% SDS-PAGE gels and immunoblotted with anti-H2a antibody (bottom panel). The rest of the lysates were immunoprecipitated (IP) with mouse anti-FLAG and goat anti-mouse IgG-agarose, subjected to 10% SDS-PAGE and immunoblotted with anti-H2a (top panel) or with anti-FLAG (middle panel). Relative amounts of H2a co-immunoprecipitated with anti-FLAG are shown relative to the total amounts below the blots. (**B**) Slower dissociation of H2a from non-palmitoylated CNX. HEK 293 cells were transfected as in A. At 2 days post-transfection the cells were pulse-labeled for 20 min with [^{35}S]-Cys and chased for the indicated times in the presence of the proteasome inhibitor MG-132. After the pulse (0 h chase) or the chase periods, the cells were lysed, H2a was immunoprecipitated from 15% of the cell lysates (right panels) and the remainders were immunoprecipitated with anti-FLAG antibody followed by elution and re-immunoprecipitation with anti-H2a, as described in the Materials and Methods (left panels). Control antibody was used instead of anti-FLAG in a control sample (Cont.). All immunoprecipitates were separated by 12% SDS-PAGE followed by phosphorimaging. For the pulse samples, two bands can be seen for H2a precursor molecules, the lower ones correspond to underglycosylated species (one of the glycosylation sites unoccupied). The fully glycosylated species shifts progressively to a faster migration because of the trimming of mannose residues on its N-glycans. The graph shows the percentage of H2a coimmunoprecipitated with CNX WT and CNX CCAA normalized to total amounts (IP anti-H2a), after chase relative to the pulse, from phosphorimager quantifications of the gels, average of three independent experiments (mean±s.e.m.). (**C**–**F**) Increased ERAD substrate colocalization at the juxtanuclear ERQC, with CNX CCAA as compared with CNX WT upon proteasomal inhibition. Plasmids encoding for H2a linked to monomeric RFP (H2a–RFP) and FLAG-tagged CNX WT (C,D) or CNX CCAA (E,F) were cotransfected in NIH 3T3 cells. At 1 day after transfection cells were incubated for 3 h in the absence (C,E) or presence of 25 μM Lac (D,F), fixed, permeabilized and incubated with mouse anti-FLAG and Cy2-conjugated goat-anti-mouse IgG. The samples were analyzed in an LSM confocal microscope. Representative confocal optical slices are shown. Scale bar: 10 μm. Manders coefficients: 0.77 for CNX wild-type, 0.88 for CNX CCAA (from 21 cells).

localization to the MAM (Lynes et al., 2012). However, our results also reinforce the close relationship between ER folding assistants and the control of mitochondrial metabolism (Simmen et al., 2010). In our specific example, calnexin expression and its reversible palmitoylation are required to allow the ER to properly signal via Ca^{2+} towards mitochondria. It is apparently owing to the presence of palmitoylated calnexin that the ER can signal a state of stress to mitochondria, probably to alleviate the accumulation of unfolded proteins within the ER (Bravo et al., 2011). However, this function is also crucial for mitochondria metabolism, as suggested by the abnormally high mitochondria membrane potential in the absence of palmitoylated calnexin. Surprisingly, our results contradict previous reports that calnexin acts as an inhibitor of SERCA2b in *Xenopus* oocytes: direct measurement of ER Ca^{2+} with aequorin suggests that the basis of our effects is an increased activity of SERCA2b in the presence of palmitoylatable calnexin, but not of the non-palmitoylated calnexin CCAA mutant (Fig. 4B). A potential explanation for

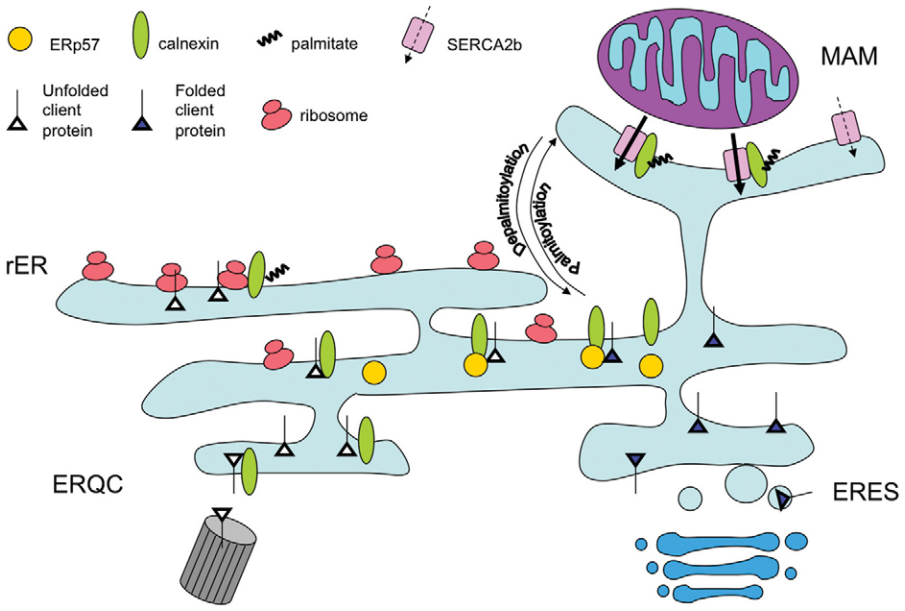

Fig. 7. Model for the calnexin shuttling between Ca^{2+} signaling and quality control. Palmitoylated calnexin interacts with SERCA on the MAM to regulate ER Ca^{2+} signaling and, to a lesser extent, on the rough ER (rER) with the translocon. Non-palmitoylated calnexin interacts with ERp57 on the rER to mediate protein folding and quality control. Additionally, non-palmitoylated calnexin can interact with ERAD substrates on the ERQC. Palmitoylation redirects chaperoning calnexin back to its role in Ca^{2+} signaling.

this discrepancy could lie in special properties of *Xenopus* oocytes or in the determination of the influence of calnexin on SERCA2b via the measurement of cytosolic Ca^{2+} waves following calnexin overexpression, as used in the earlier study (Roderick et al., 2000), rather than direct measurements of ER Ca^{2+} or assays of ER–mitochondria Ca^{2+} cross-talk.

Despite this rather marked difference in ER Ca^{2+} content, we have, however, not been able to detect differences in the induction of the unfolded protein response that are dependent on the presence or absence of calnexin (supplementary material Fig. S3D). This is consistent with earlier findings on calnexin-knockout cells (Coe et al., 2008). Rather, our findings confirm the paramount role the ER plays in the regulation of mitochondria metabolism, as elegantly demonstrated by Foskett and colleagues (Cárdenas et al., 2010).

Although the enzyme that palmitoylates calnexin has been identified as DHHC6 (Lakkaraju et al., 2012), our results predict that depalmitoylation enzymes of the thioesterase family are probably also important regulators of the ER stress response (Baekkeskov and Kanaani, 2009). However, because the APT inhibitor palmostatin B (Rusch et al., 2011) did not influence our observations (data not shown), it has to be yet unknown thioesterases that mediate calnexin shuttling between the MAM and the ER. Given the demonstrated efficacy of interference with the ER stress response in various clinical applications (Wang and Kaufman, 2012), interference with ER protein palmitoylation now provides a new therapeutic avenue with new characteristics and opportunities.

Materials and Methods

Antibodies and reagents

All chemicals were from Sigma (Oakville, ON) except Optiprep (Axis Shield, Norton, MA) and lactacystin (EMD Millipore, Billerica, MA). Rainbow [^{14}C]-labeled methylated protein standards were obtained from GE Healthcare (Little Chalfont, Buckinghamshire, UK). Promix cell labeling mix ([^{35}S]Met plus [^{35}S]Cys), (>1000 Ci/mmol) was from PerkinElmer Life and Analytical Sciences (Boston, MA). Protein-A–Sepharose was from Repligen (Needham, MA). The antibodies have been purchased as follows: mouse anti-ERp57 (StressMarq, Victoria, BC), mouse and rabbit anti-FLAG (Rockland, Gilbertsville, PA; Sigma, Oakville, ON), mouse anti-SERCA2b (EMD Millipore, Billerica, MA), mouse anti-tubulin (Sigma, St Louis, MO), rabbit anti-LDLR (Biovision, Milpitas, CA), goat anti-FACL4 (Abcam, Cambridge, UK), mouse anti-PDI (Thermo-Pierce, Rockford, IL), mouse anti-complex-2 (Mitosciences, Eugene, OR), rabbit anti-calnexin antibody (Lynes et al., 2012). The anti-phospho-calnexin antibodies were from Abcam (P563 dog, P583 human, respectively) or generated by 21st Century Biochemicals (Marlboro, MA) on behalf of us (P534, P544 dog). Goat anti-mouse IgG conjugated to agarose was from Sigma. Goat anti-mouse and anti-rabbit secondary fluorescent antibodies were from Life Technologies (Carlsbad, CA). The rabbit polyclonal anti-H2a carboxyterminal antibody was as used in earlier studies (Tolchinsky et al., 1996). Goat anti-mouse IgG antibody conjugated to Cy2 was from Jackson Labs (West Grove, PA).

Cell culture and transfections

HeLa, mouse embryonic fibroblasts (MEFs) and human embryonic kidney (HEK) 293 cells were grown in DMEM plus 10% fetal calf serum (FCS) and NIH 3T3 cells in DMEM plus 10% new born calf serum. All cells were grown at 37℃ under an atmosphere of 5% CO_2. HeLa cells were transiently transfected with Metafectene (Biontex, Martinsried, Germany). Transient transfection of NIH 3T3 cells was performed using an MP-100 Microporator (Digital Bio) according to the manufacturer's instructions. Transient transfection of HEK 293 cells was performed according to the Ca^{2+} phosphate method. The experiments were performed 24–48 h after transfection.

Biotin labeling and pulldown of surface proteins

Cells were washed twice with cold PBS with Ca^{2+} and Mg^{2+} (PBS++) and then incubated with 0.3 mg/ml EZ Link Sulfo-NHS-LC-Biotin (Thermo-Pierce, Rockford, IL) in cold PBS++ for 30 minutes on ice at 4℃. The biotinylation reaction was then quenched for 5 minutes with 50 mM glycine in PBS++, and rinsed twice with cold PBS. The cells were then lysed in mRIPA buffer with Complete protease inhibitors (Roche, Basel, Switzerland) and scraped into microcentrifuge tubes. Post-nuclear supernatants were obtained by centrifuging the lysates at 800 ***g*** for 5 minutes at 4℃. In parallel, lysates of non-biotinylated cells from each experimental condition were prepared as above. The biotinylated samples were then incubated at 4℃ overnight on a rocker with 25 µl of 40% streptavidin–agarose beads (Sigma, St Louis, MO) prepared in PBS. The beads were washed once with PBS, resuspended in Laemmli buffer and heated at 100℃ for 5 minutes. The lysates of the non-biotinylated cells were denatured in a similar manner. All samples were then analyzed by SDS-PAGE and western blotting.

Detection of palmitoylation by click chemistry

HeLa cells transfected for 48 h with FLAG–calnexin were treated with tunicamycin (10 µM) or DTT (2 mM) for 4 h. Next, cells were labeled with 100 µM alkynyl-palmitate or palmitate conjugated to BSA for 3 h. Cells were harvested in 0.1% SDS-RIPA buffer (containing CPI protease inhibitor, EDTA-free, Roche, Laval, QC) and calnexin was immunoprecipitated using the anti-FLAG antibody (Rockland). The 'click' reaction was then carried out on the immunoprecipitated labeled proteins by incubating them for 30 minutes at 37℃ with 2 mM TBTA, 50 mM $CuSO_4$, 50 mM TCEP and 2 mM Biotin-azide. Duplicate samples were then separated by SDS-PAGE, and transferred onto PVDF membranes, which were washed with either 0.1 M Tris-HCl pH 7.0 or 0.1 M

KOH. This alkali treatment removes fatty acids incorporated into proteins via thioester bonds but not via amide bonds and contributes to ensuring the specificity of the signal. Palmitoylation was detected by probing both membranes with HRP-conjugated Neutravidin using ECL.

Immunofluorescence microscopy

HeLa cells were treated with tunicamycin (10 μM) or thapsigargin (1.5 μM) for 4 h, and immunofluorescence microscopy was performed using the indicated primary antibodies, according to the protocol described previously (Gilady et al., 2010). LDLR surface binding was detected by binding of a 1:100 dilution of anti-LDLR antibody in DMEM, 10% FBS and 1% BSA. Intracellular FLAG-tagged calnexin was detected after permeabilization with 1% Triton X-100. The procedures employed with NIH 3T3 cells were as described previously (Avezov et al., 2008; Kamhi-Nesher et al., 2001). Confocal microscopy was performed on a Zeiss laser scanning confocal microscope (LSM 510; Carl Zeiss, Jena, Germany) as described previously (Avezov et al., 2008). Colocalization analysis (Manders) was performed using ImageJ and Imaris software.

Co-immunoprecipitation experiments

Cells were washed twice with PBS++ and incubated for 30 minutes at room temperature with 2 mM Dithiobis (succinimidyl proprionate) (Thermo Scientific, Rockford, IL) in PBS++ to crosslink interacting proteins. The cells were then washed twice more and incubated in 10 mM NH_4Cl in PBS++ for 10 minutes to quench the crosslinking reaction. The cells were then washed a final time in PBS++ and harvested in CHAPS lysis buffer (1% CHAPS, 10 mM Tris pH 7.4, 150 mM NaCl, 1 mM EDTA) containing Complete protease inhibitors (Roche, Basel, Switzerland). Post-nuclear supernatants were obtained by centrifuging the lysates for 5 minutes at 4℃ at 800 ***g***, and were subsequently incubated with the indicated antibodies for 1 h at 4℃ on a rocker. Protein-A–Sepharose beads were then added and the lysates incubated for a further 1 h. The beads were then washed three times in CHAPS buffer and resuspended in Laemmli buffer and analyzed by SDS-PAGE and western blotting. For immunoprecipitation from HEK 293 cells, cell lysis was performed in 2% sodium cholate for 30 min on ice, and debris and nuclei were pelleted in a microfuge for 30 minutes at 4℃. The samples were immunoprecipitated with anti-FLAG and goat anti-mouse-IgG–agarose overnight, followed by washes and elution by boiling with sample buffer containing β-mercaptoethanol.

Metabolic labeling

Subconfluent (90%) cell monolayers in 100-mm dishes were labeled with [^{35}S]Cys. Co-immunoprecipitation with anti-calnexin antibody was performed as described previously (Frenkel et al., 2004). Briefly, after metabolic labeling, cells were lysed in HBS buffer pH 7.5, containing 2% sodium cholate, cell lysates were immunoprecipitated with anti-FLAG antibody, boiled in 1% SDS, then diluted with 10 volumes of 1% Triton X-100, 0.5% sodium deoxycholate in HBS and reimmunoprecipitated with anti-H2a antibody. SDS-PAGE gels were analyzed by fluorography using 20% 2,5-diphenyloxazole and were exposed to Biomax MS film using a transcreen-LE from Kodak (Vancouver, BC). Quantification was performed in a Fujifilm FLA 5100 phosphorimager (Japan).

Reverse transcriptase PCR to assay the unfolded protein response

Calnexin-knockout cells transfected as indicated were treated with 1.5 μM thapsigargin for 16 h or left as controls. Total RNA was isolated using TRIzol (Life Technologies, Carlsbad, CA) and amplified with primers for Xbp-1 (5′-CCTTGTGGTTGAGAACCAGG-3′ and 5′-CTAGAGGCTTGGTGTATAC-3′) and GAPDH, respectively (5′-AACTTTGGCATTGTGGAAGG-3′ and 5′-ACACATTGGGGGTAGGAACA-3′). PCR products were separated on 7.5% and 1% acrylamide gels, respectively.

Plasmid-based ER and mitochondria Ca^{2+} measurements

ER Ca^{2+} was measured with pHSVerAEQ (gift from Javier Alvarez, Valladolid, Spain). Cells were transfected with this plasmid (and constructs expressing calnexin as indicated) and processed for measurements 24 h following transfection as published (Alvarez and Montero, 2002). Following the depletion of ER Ca^{2+} with 0.5 mM EGTA and 1 μM 2,5-di-tert-butyl-benzohydroquinone (Sigma), aequorin was reconstituted with 10 μM coelenterazine hcp (Sigma). After leaving the cells for 1 h at room temperature in the dark, cells were perfused with medium containing 1 mM Ca^{2+}. Luminescence from this condition and total luminescence following digitonin permeabilization was assayed on a Lumat luminometer (Berthold, Bad Wildbad, Germany). For mitochondrial Ca^{2+}, mitochondrially targeted R-GECO1 was used (Zhao et al., 2011). Calnexin wild-type and knockout MEFs were transfected with a plasmid encoding mitochondrial R-GECO1, whose fluorescence was measured on a Olympus Fluoview FV1000 microscope and quantified using the FV10-ASW 3.1 software (Olympus, Richmond Hill, ON). Fluorescence measurements were initialized after establishment of a baseline, followed by the addition of 1 μM thapsigargin.

Construction of mitochondria-targeted R-GECO1 plasmid

To construct a plasmid expressing mitochondria-targeted R-GECO1, the gene for R-GECO1 in pTorPE[1] was used as a template. PCR was carried out by using primers: 'GCaMP_FW_BamH1_mito' (5′-GAGGATCCAACCATGGTCGACT-CATCACGTC-3′) and 'GCaMP_RV_HindIII' (5′-CGCAAGCTTCTACTTC-GCTGTCATCATTTGTAC-3′). PCR products were purified using 1% agarose gel (Agarose S, Nippon Gene Co.) electrophoresis. DNA was extracted from the appropriate gel slice using the GeneJet DNA Purification Kit (Thermo Scientific). The PCR product was then digested with *Bam*H1 and *Hin*dIII (Thermo Scientific), repurified as described above, and ligated into the the CMV-mito-GEM-GECO1[1] vector previously digested with the same restriction enzymes. The resulting ligation products were transformed into DH10B *E. coli* by electroporation, and the transformed *E. coli* were grown on agar plates (with 400 μg/ml ampicillin) overnight. *E. coli* colonies on agar plates were then picked up and cultured in LB medium (with 100 μg/ml ampicillin, 250 rpm shaking) for 12 to 16 h. DNA plasmid purification was performed using the GeneJET Plasmid Miniprep Kit (Thermo Scientific), and the purified mitochondria-targeting R-GECO1 DNA plasmids were verified by sequencing at the University of Alberta Molecular Biology Services Unit.

Flow cytometry

Cells were loaded with either 1 μM Fluo8 (AAT Bioquest, Sunnyvale, CA), 1 μM Rhod2 (Life Technologies, Carlsbad, CA) or 20 nM TMRM (Sigma, St Louis, MO) and incubated in DMEM (Life Technologies, Carlsbad, CA) for 30 minutes at 37℃. Cells were then harvested in HEPES-buffered saline (0.1% glucose, 0.1% BSA) and subjected to flow cytometry using a FACS Scan cytometer (BD Biosciences, Mississauga, ON) before treatment and 10 (50 μM histamine) or 20 seconds (1.5 μM thapsigargin) after drug administration.

Optiprep gradient fractionations

HeLa cells were treated with the indicated stressors and then washed twice in PBS++ and collected in mitochondria homogenization buffer (10 mM HEPES pH 7.4, 250 mM sucrose, 1 mM EDTA, 1 mM EGTA). The cell suspension was passed through an 18 μM clearance ball-bearing homogenizer (Isobiotech, Heidelberg, Germany) 15 times. The cells were subsequently centrifuged for 10 minutes at 800 ***g*** at 4℃, to pellet nuclei and unbroken cells. The supernatant was layered over a 10–30% continuous gradient of Optiprep density gradient medium (Axis-Shield, Norton, MA), and was centrifuged in an SW55 Ti rotor (Beckman Coulter, Mississauga, ON) for 3 h at 32,700 rpm. Fractions were taken from the top of the gradient and analyzed by SDS-PAGE and western blotting.

Acknowledgements

We thank Marek Michalak for helpful discussions. We especially thank Klaus Ballanyi for help with the supplementary material. The plasmid encoding ER-targeted aequorin was a generous gift from Javier Alvarez, Valladolid, Spain.

Author contributions

E.M.L. participated in the experimental design, performed experiments and data analysis, and participated in the design of the figures as well as the writing of the manuscript; A.R. performed the Ca^{2+} measurements in Fig. 4A–D; M.S. performed the quality control experiments in Fig. 6; C.O.S. performed heavy and light membrane fractionations in supplementary material Fig. S3A and S5A; M.C.Y. assisted with the 'click chemistry'; J.W. constructed the R-GECO1 plasmid used in supplementary material Fig. S3B; A.J. performed the UPR RT-PCR in Fig. S3D; N.M. performed heavy and light membrane fractionations in Figure 1A; M.D.B. performed additional fractionations; R.E.C. helped design the R-GECO1 plasmid; L.G.B assisted with 'click chemistry' and manuscript editing; G.Z.L. directed and designed the ERQC experiments and wrote the corresponding section of the manuscript; and T.S. directed the project, performed the immunofluorescence experiments in Fig. 1C and wrote the manuscript.

Funding

This work is supported by the Alberta Cancer Foundation [grant number 25018]; the Canadian Cancer Society Research Institute [grant number 2010-700306; and the Alberta Innovates Health Solutions (scholarship 200500396); E.M.L. was supported by Alberta Cancer Foundation (studentships 24136 and 25370); R.E.C. is a Tier II Canada Research Chair in Bioanalytical

Chemistry and is supported by Canadian Institutes of Health Research (CIHR) [grant number NHG 99085]; L.G.B. was supported by CIHR [grant number MOP 81248] and the Alberta Cancer Research Institute (ACRI) [grant number 24425]; G.Z.L. is supported by the Israel Science Foundation [grant number 1070/10].

Supplementary material available online at
http://jcs.biologists.org/lookup/suppl/doi:10.1242/jcs.125856/-/DC1

References

Alvarez, J. and Montero, M. (2002). Measuring [Ca2+] in the endoplasmic reticulum with aequorin. *Cell Calcium* **32**, 251-260.

Arnaudeau, S., Kelley, W. L., Walsh, J. V., Jr and Demaurex, N. (2001). Mitochondria recycle Ca(2+) to the endoplasmic reticulum and prevent the depletion of neighboring endoplasmic reticulum regions. *J. Biol. Chem.* **276**, 29430-29439.

Avezov, E., Frenkel, Z., Ehrlich, M., Herscovics, A. and Lederkremer, G. Z. (2008). Endoplasmic reticulum (ER) mannosidase I is compartmentalized and required for N-glycan trimming to Man5-6GlcNAc2 in glycoprotein ER-associated degradation. *Mol. Biol. Cell* **19**, 216-225.

Baekkeskov, S. and Kanaani, J. (2009). Palmitoylation cycles and regulation of protein function (Review). *Mol. Membr. Biol.* **26**, 42-54.

Baldwin, A. C., Green, C. D., Olson, L. K., Moxley, M. A. and Corbett, J. A. (2012). A role for aberrant protein palmitoylation in FFA-induced ER stress and β-cell death. *Am. J. Physiol.* **302**, E1390-E1398.

Bravo, R., Vicencio, J. M., Parra, V., Troncoso, R., Munoz, J. P., Bui, M., Quiroga, C., Rodriguez, A. E., Verdejo, H. E., Ferreira, J. et al. (2011). Increased ER-mitochondrial coupling promotes mitochondrial respiration and bioenergetics during early phases of ER stress. *J. Cell Sci.* **124**, 2143-2152.

Cárdenas, C., Miller, R. A., Smith, I., Bui, T., Molgó, J., Müller, M., Vais, H., Cheung, K. H., Yang, J., Parker, I. et al. (2010). Essential regulation of cell bioenergetics by constitutive InsP3 receptor Ca2+ transfer to mitochondria. *Cell* **142**, 270-283.

Chevet, E., Wong, H. N., Gerber, D., Cochet, C., Fazel, A., Cameron, P. H., Gushue, J. N., Thomas, D. Y. and Bergeron, J. J. (1999). Phosphorylation by CK2 and MAPK enhances calnexin association with ribosomes. *EMBO J.* **18**, 3655-3666.

Coe, H. and Michalak, M. (2010). ERp57, a multifunctional endoplasmic reticulum resident oxidoreductase. *Int. J. Biochem. Cell Biol.* **42**, 796-799.

Coe, H., Bedard, K., Groenendyk, J., Jung, J. and Michalak, M. (2008). Endoplasmic reticulum stress in the absence of calnexin. *Cell Stress Chaperones* **13**, 497-507.

Csordás, G., Renken, C., Várnai, P., Walter, L., Weaver, D., Buttle, K. F., Balla, T., Mannella, C. A. and Hajnóczky, G. (2006). Structural and functional features and significance of the physical linkage between ER and mitochondria. *J. Cell Biol.* **174**, 915-921.

de Brito, O. M. and Scorrano, L. (2008). Mitofusin 2 tethers endoplasmic reticulum to mitochondria. *Nature* **456**, 605-610.

Delom, F., Fessart, D. and Chevet, E. (2007). Regulation of calnexin sub-cellular localization modulates endoplasmic reticulum stress-induced apoptosis in MCF-7 cells. *Apoptosis* **12**, 293-305.

Dowal, L., Yang, W., Freeman, M. R., Steen, H. and Flaumenhaft, R. (2011). Proteomic analysis of palmitoylated platelet proteins. *Blood* **118**, e62-e73.

Ferrera, D., Panigada, M., Porcellini, S. and Grassi, F. (2008). Recombinase-deficient T cell development by selective accumulation of CD3 into lipid rafts. *Eur. J. Immunol.* **38**, 1148-1156.

Frenkel, Z., Shenkman, M., Kondratyev, M. and Lederkremer, G. Z. (2004). Separate roles and different routing of calnexin and ERp57 in endoplasmic reticulum quality control revealed by interactions with asialoglycoprotein receptor chains. *Mol. Biol. Cell* **15**, 2133-2142.

Gilady, S. Y., Bui, M., Lynes, E. M., Benson, M. D., Watts, R., Vance, J. E. and Simmen, T. (2010). Ero1alpha requires oxidizing and normoxic conditions to localize to the mitochondria-associated membrane (MAM). *Cell Stress Chaperones* **15**, 619-629.

Glancy, B. and Balaban, R. S. (2012). Role of mitochondrial Ca2+ in the regulation of cellular energetics. *Biochemistry* **51**, 2959-2973.

Hayashi, T. and Su, T. P. (2007). Sigma-1 receptor chaperones at the ER-mitochondrion interface regulate Ca(2+) signaling and cell survival. *Cell* **131**, 596-610.

Higo, T., Hattori, M., Nakamura, T., Natsume, T., Michikawa, T. and Mikoshiba, K. (2005). Subtype-specific and ER lumenal environment-dependent regulation of inositol 1,4,5-trisphosphate receptor type 1 by ERp44. *Cell* **120**, 85-98.

Jessop, C. E., Chakravarthi, S., Garbi, N., Hämmerling, G. J., Lovell, S. and Bulleid, N. J. (2007). ERp57 is essential for efficient folding of glycoproteins sharing common structural domains. *EMBO J.* **26**, 28-40.

Kamhi-Nesher, S., Shenkman, M., Tolchinsky, S., Fromm, S. V., Ehrlich, R. and Lederkremer, G. Z. (2001). A novel quality control compartment derived from the endoplasmic reticulum. *Mol. Biol. Cell* **12**, 1711-1723.

Kang, R., Wan, J., Arstikaitis, P., Takahashi, H., Huang, K., Bailey, A. O., Thompson, J. X., Roth, A. F., Drisdel, R. C., Mastro, R. et al. (2008). Neural palmitoyl-proteomics reveals dynamic synaptic palmitoylation. *Nature* **456**, 904-909.

Kondratyev, M., Avezov, E., Shenkman, M., Groisman, B. and Lederkremer, G. Z. (2007). PERK-dependent compartmentalization of ERAD and unfolded protein response machineries during ER stress. *Exp. Cell Res.* **313**, 3395-3407.

Kraus, A., Groenendyk, J., Bedard, K., Baldwin, T. A., Krause, K. H., Dubois-Dauphin, M., Dyck, J., Rosenbaum, E. E., Korngut, L., Colley, N. J. et al. (2010). Calnexin deficiency leads to dysmyelination. *J. Biol. Chem.* **285**, 18928-18938.

Lakkaraju, A. K., Abrami, L., Lemmin, T., Blaskovic, S., Kunz, B., Kihara, A., Dal Peraro, M. and van der Goot, F. G. (2012). Palmitoylated calnexin is a key component of the ribosome-translocon complex. *EMBO J.* **31**, 1823-1835.

Lederkremer, G. Z. (2009). Glycoprotein folding, quality control and ER-associated degradation. *Curr. Opin. Struct. Biol.* **19**, 515-523.

Leitman, J., Ron, E., Ogen-Shtern, N. and Lederkremer, G. Z. (2013). Compartmentalization of endoplasmic reticulum quality control and er-associated degradation factors. *DNA Cell Biol.* **32**, 2-7.

Li, G., Mongillo, M., Chin, K. T., Harding, H., Ron, D., Marks, A. R. and Tabas, I. (2009). Role of ERO1-alpha-mediated stimulation of inositol 1,4,5-triphosphate receptor activity in endoplasmic reticulum stress-induced apoptosis. *J. Cell Biol.* **186**, 783-792.

Lynes, E. M., Bui, M., Yap, M. C., Benson, M. D., Schneider, B., Ellgaard, L., Berthiaume, L. G. and Simmen, T. (2012). Palmitoylated TMX and calnexin target to the mitochondria-associated membrane. *EMBO J.* **31**, 457-470.

Myhill, N., Lynes, E. M., Nanji, J. A., Blagoveshchenskaya, A. D., Fei, H., Carmine Simmen, K., Cooper, T. J., Thomas, G. and Simmen, T. (2008). The subcellular distribution of calnexin is mediated by PACS-2. *Mol. Biol. Cell* **19**, 2777-2788.

Oliver, J. D., van der Wal, F. J., Bulleid, N. J. and High, S. (1997). Interaction of the thiol-dependent reductase ERp57 with nascent glycoproteins. *Science* **275**, 86-88.

Raturi, A. and Simmen, T. (2013). Where the endoplasmic reticulum and the mitochondrion tie the knot: the mitochondria-associated membrane (MAM). *Biochim. Biophys. Acta*. **1833**, 213-224.

Rizzuto, R., Marchi, S., Bonora, M., Aguiari, P., Bononi, A., De Stefani, D., Giorgi, C., Leo, S., Rimessi, A., Siviero, R. et al. (2009). Ca(2+) transfer from the ER to mitochondria: when, how and why. *Biochim. Biophys. Acta* **1787**, 1342-1351.

Roderick, H. L., Lechleiter, J. D. and Camacho, P. (2000). Cytosolic phosphorylation of calnexin controls intracellular Ca(2+) oscillations via an interaction with SERCA2b. *J. Cell Biol.* **149**, 1235-1248.

Ruddock, L. W. and Molinari, M. (2006). N-glycan processing in ER quality control. *J. Cell Sci.* **119**, 4373-4380.

Rusch, M., Zimmermann, T. J., Bürger, M., Dekker, F. J., Görmer, K., Triola, G., Brockmeyer, A., Janning, P., Böttcher, T., Sieber, S. A. et al. (2011). Identification of acyl protein thioesterases 1 and 2 as the cellular targets of the Ras-signaling modulators palmostatin B and M. *Angew. Chem. Int. Ed. Engl.* **50**, 9838-9842.

Rutkevich, L. A. and Williams, D. B. (2011). Participation of lectin chaperones and thiol oxidoreductases in protein folding within the endoplasmic reticulum. *Curr. Opin. Cell Biol.* **23**, 157-166.

Shenkman, M., Ayalon, M. and Lederkremer, G. Z. (1997). Endoplasmic reticulum quality control of asialoglycoprotein receptor H2a involves a determinant for retention and not retrieval. *Proc. Natl. Acad. Sci. USA* **94**, 11363-11368.

Simmen, T., Lynes, E. M., Gesson, K. and Thomas, G. (2010). Oxidative protein folding in the endoplasmic reticulum: tight links to the mitochondria-associated membrane (MAM). *Biochim. Biophys. Acta* **1798**, 1465-1473.

Tolchinsky, S., Yuk, M. H., Ayalon, M., Lodish, H. F. and Lederkremer, G. Z. (1996). Membrane-bound versus secreted forms of human asialoglycoprotein receptor subunits. Role of a juxtamembrane pentapeptide. *J. Biol. Chem.* **271**, 14496-14503.

Wang, S. and Kaufman, R. J. (2012). The impact of the unfolded protein response on human disease. *J. Cell Biol.* **197**, 857-867.

Wieckowski, M. R., Giorgi, C., Lebiedzinska, M., Duszynski, J. and Pinton, P. (2009). Isolation of mitochondria-associated membranes and mitochondria from animal tissues and cells. *Nat. Protoc.* **4**, 1582-1590.

Zapun, A., Darby, N. J., Tessier, D. C., Michalak, M., Bergeron, J. J. and Thomas, D. Y. (1998). Enhanced catalysis of ribonuclease B folding by the interaction of calnexin or calreticulin with ERp57. *J. Biol. Chem.* **273**, 6009-6012.

Zhao, Y., Araki, S., Wu, J., Teramoto, T., Chang, Y. F., Nakano, M., Abdelfattah, A. S., Fujiwara, M., Ishihara, T., Nagai, T. et al. (2011). An expanded palette of genetically encoded Ca^{2+} indicators. *Science* **333**, 1888-1891.

Zhivotovsky, B. and Orrenius, S. (2011). Calcium and cell death mechanisms: a perspective from the cell death community. *Cell Calcium* **50**, 211-221.

Zuppini, A., Groenendyk, J., Cormack, L. A., Shore, G., Opas, M., Bleackley, R. C. and Michalak, M. (2002). Calnexin deficiency and endoplasmic reticulum stress-induced apoptosis. *Biochemistry* **41**, 2850-2858.

Fig. S1. Full gels for Figure 1B. Representations of the control gels seen in Fig. 1B for calnexin, FACL4, and PDI. Molecular weight markers are shown on the left and arrows indicate the bands of interest.

Fig. S2. Additional analysis of calnexin palmitoylation and phosphorylation. A. Optiprep fractionation following thapsigargin treatment. Homogenized HeLa cell lysates were separated via Optiprep following a 4h treatment with 1.5 μM Thapsigargin into 6 fractions. Membrane fractions were analyzed as indicated by SDS-PAGE and Western Blot for PDI (pan-ER), SERCA2b and FACL4 (MAM), as well as calnexin. **B.** Calnexin palmitoylation is reduced during DTT stress. HeLa cells were incubated for 4h with 5 mM DTT and then processed for click chemistry as described (Lynes et al., 2012). **C.** Neither calnexin palmitoylation nor the phosphorylation status of serines 554 and 564 influence serine 583 phosphorylation. Calnexin knockout (ko) MEFs and ko cells transfected with FLAG-tagged wild type CCAA, M3 (S554, 564→A), or M4 (S554, 564→D) calnexin were lysed and processed for Western blot using the phospho-serine 583 antibody.

Fig. S3. Influence of calnexin presence on mitochondria calcium import, mitochondria membrane potential and ER ability to trigger the unfolded protein response. A. Measurement of cytosolic calcium following thapsigargin-mediated ER calcium release. Calnexin knockout (ko) MEFs and ko cells transfected with FLAG-tagged wild type or CCAA calnexin were loaded with FURA-2. Cells were then treated with 1.5 μM thapsigargin and probe fluorescence was recorded before and after thapsigargin treatment by flow cytometry. The increases of fluorescence for the three conditions were not statistically different from each other. **B**. Plasmid-based measurement of mitochondrial calcium content following thapsigargin. Calnexin wildtype and knockout (ko) MEFs were transfected with a plasmid encoding mitochondria-targeted R-GECO-1. The increase in relative fluorescence units was assayed from three independent experiments following the protocol outlined in Materials and Methods. A representative curve for wild type and knockout cells is shown on the right. **C**. Measurement of mitochondrial membrane potential. Calnexin knockout (ko) MEFs and ko cells transfected with FLAG-tagged wild type or CCAA calnexin were loaded with TMRM and probe fluorescence was recorded by flow cytometry (Statistics: P=0.001 for calnexin wild type, P=0.4135 for calnexin CCAA). **D**. Xbp-1 splicing measured by reverse transcriptase PCR. Calnexin knockout (ko) MEFs and ko cells transfected with FLAG-tagged wild type or CCAA calnexin were treated with 1.5 μM thapsigargin for 16h, followed by analysis of the Xbp-1 mRNA. PCR products were separated on a 7.5% acrylamide gel for Xbp-1 and a 1% acrylamide gel for GAPDH.

Fig. S4. 2BP promotes the calnexin chaperone activity. A. Calnexin-ERp57 co-immunoprecipitation following 2BP treatment. HeLa cells were treated for 4 h with 100 μM 2BP. DSP-crosslinked lysates (5% inputs) and calnexin immunoprecipitates were analyzed for calnexin and co-immunoprecipitating ERp57. P=0.07. **B.** LDLR surface biotinylation following 2BP treatment. HeLa cells were lysed and processed for Western blot using the LDLR antibody. In parallel, the same set of cells was processed for surface biotinylation and probed for biotinylated surface LDLR.

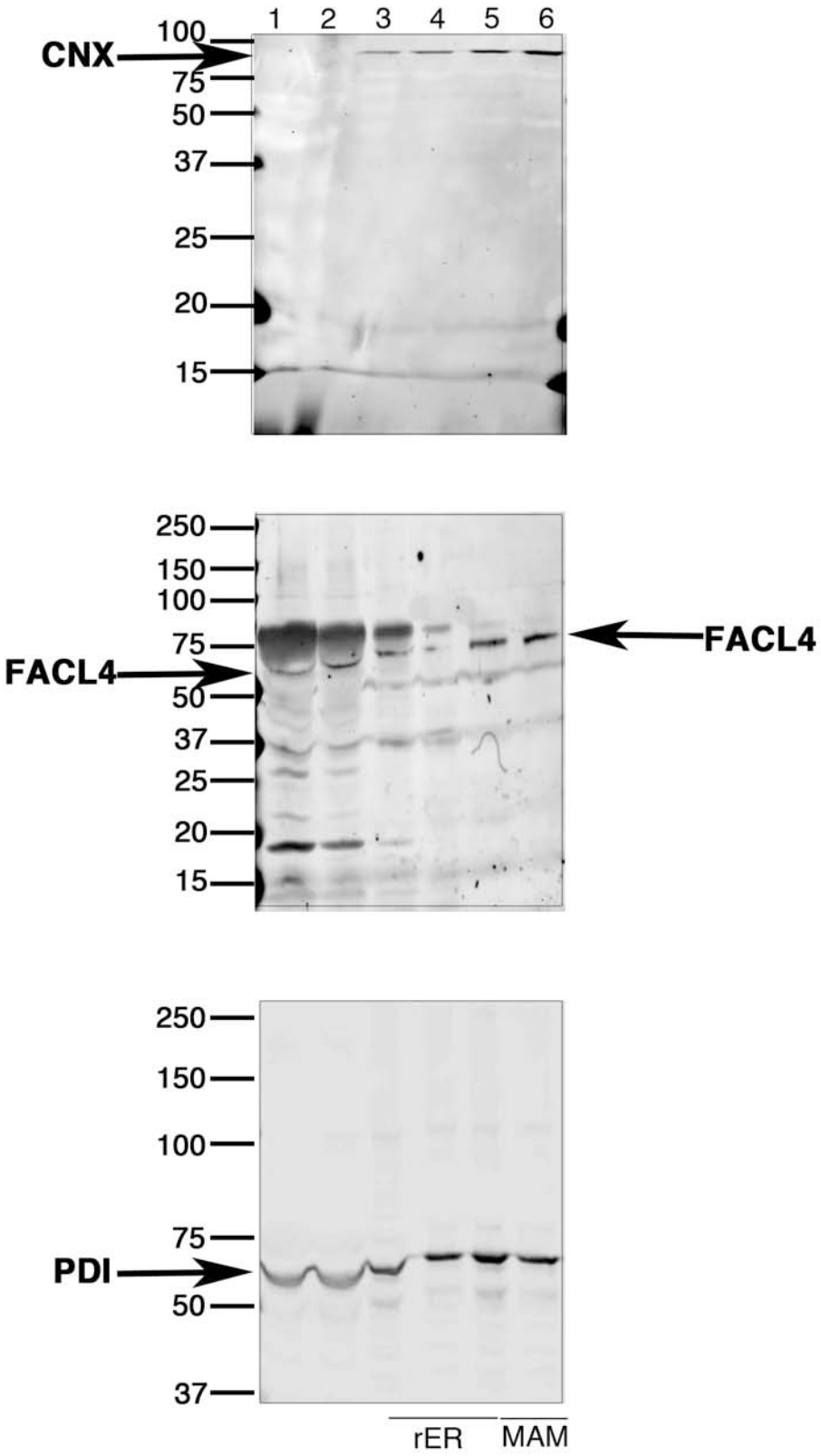

Supplemental Figure 1, Lynes et al.

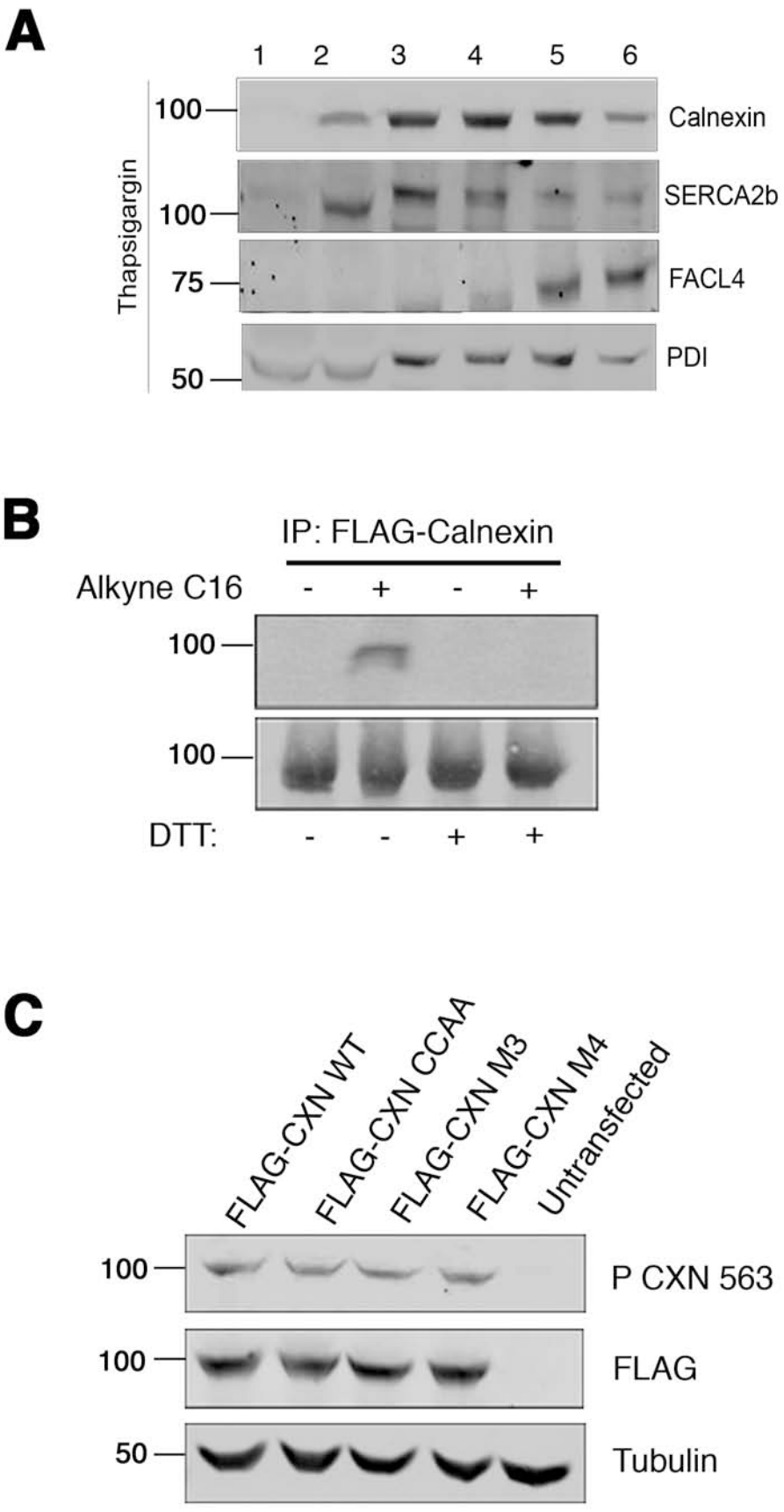

Supplemental Figure 2, Lynes et al.

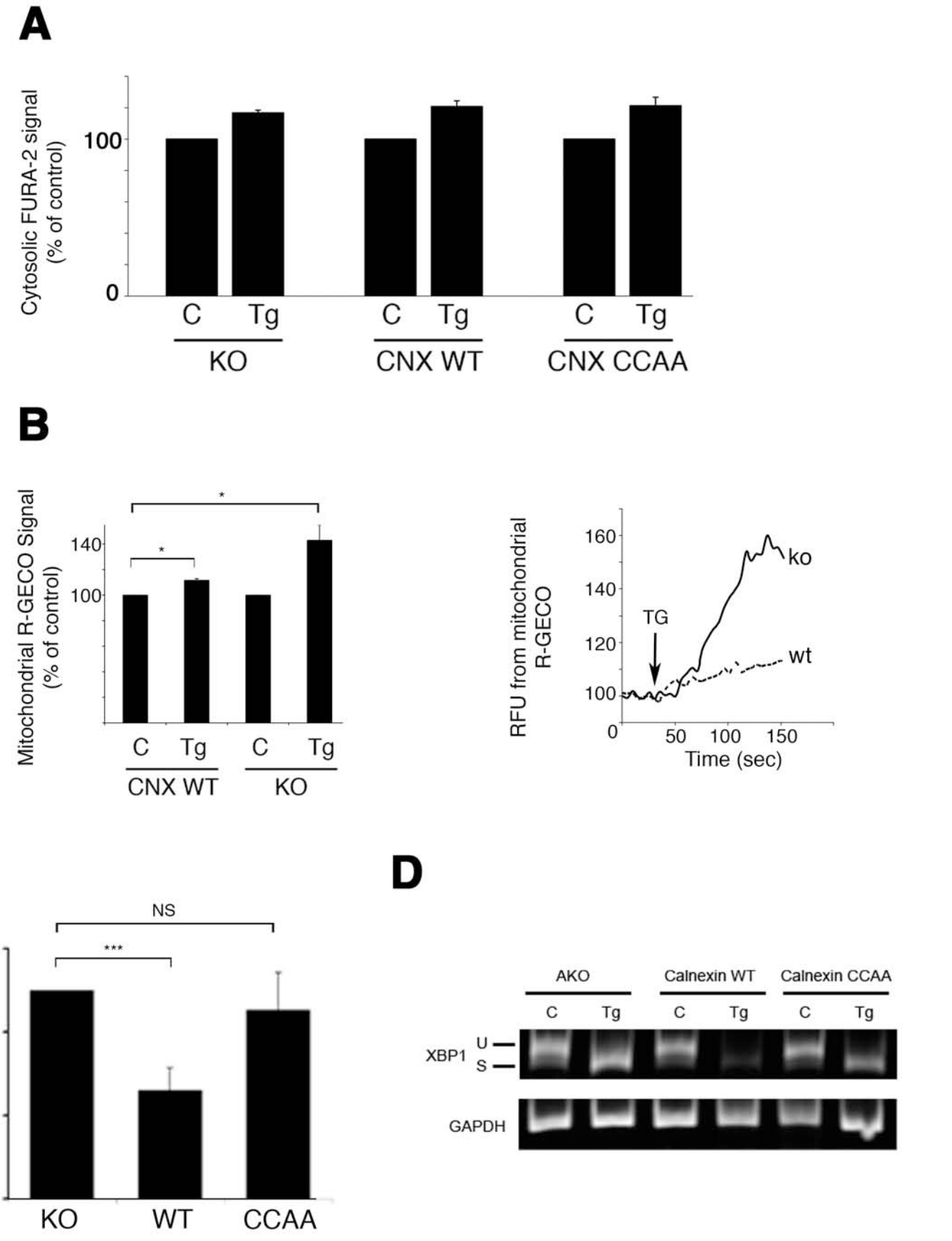

Supplemental Figure 3, Lynes et al.

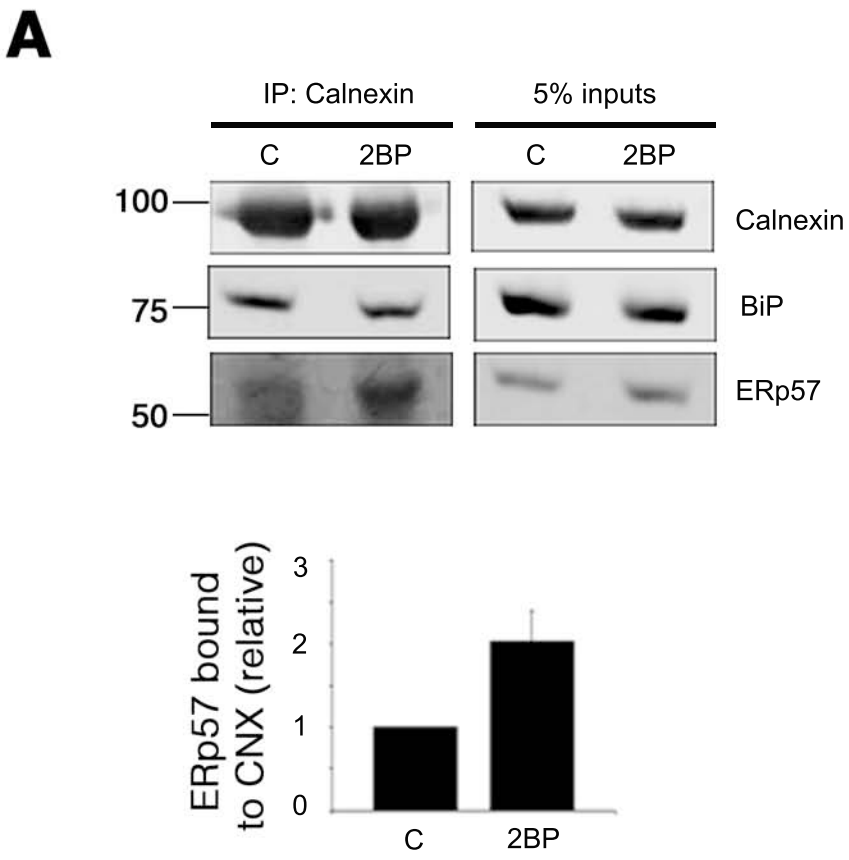

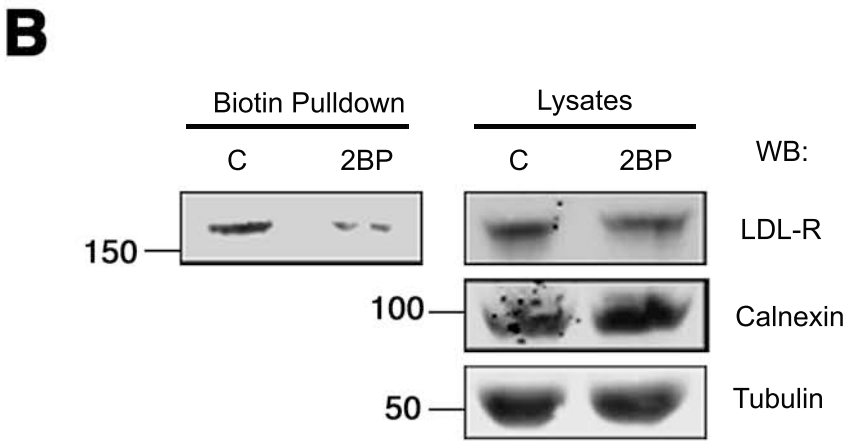

Supplemental Figure 4, Lynes et al.